Recombinant reporter phage rTUN1::*nLuc* enables rapid detection and real-time antibiotic susceptibility testing of *Klebsiella pneumoniae* K64 strains

Peter Braun[1§]*, Rene Raab[1§], Joachim J Bugert[1], Simone Eckstein[1]

[1] Bundeswehr Institute of Microbiology, Munich, Germany

[§]authors contributed equally
*Correspondence: peter3braun@bundeswehr.org

Abstract

The emergence of multi drug resistant (MDR) *Klebsiella pneumoniae* (*Kp*) strains constitutes an enormous threat to global health as MDR associated treatment failure causes high mortality rates in nosocomial infections. Rapid pathogen detection and antibiotic resistance screening is therefore crucial for successful therapy and thus, patient survival. Reporter phage-based diagnostics offer a way to speed up pathogen identification and resistance testing, as integration of reporter genes into highly specific phages allow real-time detection of phage replication and thus, living host cells. *Kp* specific phages use the host's capsule, a major virulence factor of *Kp*, as receptor for adsorption. To date, 80 different *Kp* capsule types (K-serotypes) have been described with predominant capsule types varying between different countries and continents. Therefore, reporter phages need to be customized according to the locally prevailing variants. Recently, we described the autographivirus vB_KpP_TUN1 (TUN1), which specifically infects *Kp* K64 strains, the most predominant capsule type at the military hospital in Tunis (MHT) that is also associated with high mortality rates. In this work, we developed the highly specific recombinant reporter phage rTUN1::*nLuc*, which produces Nanoluciferase (nLuc) upon host infection and thus, enables rapid detection of *Kp* K64 cells in clinical matrices such as blood and urine. At the same time, rTUN1::*nLuc* allows for rapid antibiotic susceptibility testing and therefore identification of suitable antibiotic treatment in less than 3 hours.

Introduction

The ESKAPEE bacteria (*Enterococcus faecium*, *Staphylococcus aureus*, *Klebsiella pneumoniae*, *Acinetobacter baumanni*, *Pseudomonas aeruginosa*, *Escherichia coli* and *Enterobacter* species) are responsible for the majority of nosocomial infections and typically possess multi-drug resistance (MDR). Among these, the opportunistic pathogen *K. pneumoniae* (*Kp*) poses a particular threat for public health. Ubiquitously occurring as a commensal, *Kp* can be found among gastro-intestinal microbiota, in the respiratory tract and on the skin. As a facultative pathogen, *Kp* can cause a variety of severe nosocomial diseases such as pneumonia, sepsis, wound- and urinary tract infections (UTIs). In recent years, the number of community-acquired cases of *Kp*-caused pneumonia and meningitis has dramatically increased (Herridge et al., 2020). Together with the emergence of acquired MDR against broad-spectrum antibiotics (ABs) and the natural resistances of the bacterium, treatment of *Kp*

infections has become a global healthcare challenge (Babini & Livermore, 2000; Knothe et al., 1983; Prestinaci et al., 2015).

Infections with carbapenem-resistant *Kp* are associated with serious symptoms and high mortality rates (Patel et al., 2008; Schwaber et al., 2008). Therefore, rapid diagnosis of the infection as well as detection of resistance markers are crucial for patient survival. Classical approaches to identify carbapenem-resistant *Kp* rely on bacterial cell culture with subsequent biochemical profiling and therefore provide results only after a few days. While nucleic acid based tools such as diagnostic real-time PCR or loop-mediated isothermal amplification (LAMP) enable fast and specific detection of the pathogen, the established assays mainly target carbapenem-resistance genes and therefore cannot distinguish between living cells and DNA residues present in the sample (Hartman et al., 2009; Kurupati et al., 2004; Nakano et al., 2015).

Diagnostic bacteriophages (phages) represent a promising alternative approach. In addition to their therapeutic potential, phages are suited for the identification of bacteria due to the viruses' high specificity. Phage sensitivity assays have been in practise for centuries for a variety of pathogens such as *Bacillus anthracis* (Turnbull et al., 2008) or *Yersinia pestis* (Garcia et al., 2008). Such techniques include antibody-based detection of phages using ELISA (Stewart et al., 2013) or detection of amplified phage DNA (Anany et al., 2018). Another option is to exploit the bacteriolytic activity of phages and detect released cellular components such as ATP (Blasco et al., 1998). The most promising methodology, however, is the use of reporter phages, which either have a reporter molecule directly attached to the virion surface or produced during phage replication (Goodridge et al., 1999; Hennes & Simon, 1995; Meile et al., 2020).

While most phages of gram negative bacteria utilize surface structures such as lipopolysaccharides (LPS), teichoic acids or proteins as host receptors for adsorption (Nobrega et al., 2018), the specificity of *Kp* phages is mostly determined by the different *Kp* capsule polysaccharides (CPS). CPS represent a major virulence factor of *Kp* as the thick layer protects the bacterial cell from phagocytosis and prevents complement binding during host response. In addition, the CPS forms a physical barrier towards ABs as it hampers diffusion into the bacterial cell (Domenico et al., 1994; Merino et al., 1992; Shon et al., 2013). To date, about 80 different *Kp* capsule serotypes (K-types) have been described (Pan et al., 2015). Since *Kp* specific phages are usually capable of infecting only one or a few capsule types, the selection of a suitable reporter phage is crucial for reliable diagnostics. As predominant capsule types vary from region to region, reporter phages need to be customized according to the locally prevailing variant. In Tunisia, e.g., the majority of nosocomial infections at the Military Hospital of Instructions in Tunis (MHT) are caused by a *Kp* strain featuring capsule type 64 (K64). These *Kp* K64

70 infections are associated with high mortality rates, especially among intensive care patients (Eckstein
71 et al., 2021).
72 In this study, we genetically engineered the recently identified *Kp* K64-specific phage vB_KpP_TUN1
73 (TUN1), and constructed a recombinant TUN1 reporter phage (rTUN1::*nLuc*) for the rapid detection of
74 *Kp* K64 strains in bacterial cell culture or directly from clinically relevant matrices as well as for
75 conducting real-time antibiotic susceptibility testing.
76

77 ## Material and Methods

78 **Bacterial growth**

79 All *K. pneumoniae* and *E. coli* strains were cultivated in LB-broth [10% NaCl (w/v), 10% peptone (w/v),
80 5% yeast extract (w/v)] at 37° C under constant shaking.

81 ***In vitro* DNA-Assembly of synthetic phage genomes**

82 For isolation of genomic DNA (gDNA) of phages Master-Pure™ Complete DNA and RNA Purification Kit
83 (Lucigen, Wisconsin, USA) was used according to the supplier's protocol. Prior to assemble the
84 synthetic TUN1 WT genome, TUN1 WT gDNA was used as PCR template to amplify five fragments. This
85 was achieved by using the primer pairs TUN1 F1 + R1 (= Fragment 1), TUN1 F2 + R2 (= Fragment 2),
86 TUN1 F3 + R3 (= Fragment 3), TUN1 F4 + R4 (= Fragment 4) and TUN1 F5 + R5 (= Fragment 5). Primers
87 were designed to generate 15-25 bp overlaps between adjacent fragments to ensure efficient
88 assembly. The circular approach was done in the same way, with the difference of replacing Fragment
89 1 and Fragment 5 by Fragment 5_1, amplified using the primers TUN1 F5 + R1 (Supplementary Figure
90 S1A).

91 If not stated differently, the four TUN1 fragments of the circular approach described above were used
92 for all further TUN1 DNA assemblies.

93 In order to generate the deletion strain TUN1 Δhpgc1, Fragment 5_1 was replaced by Fragment 5_1
94 gp1 (using the primer pair TUN1 F5 + gp1 R) and Fragment 2 by Fragment 2 gp5 (primers TUN1 gp5 F
95 and 2R). TUN1 Δhpgc2 was achieved by using Fragment 5_1 gp6 (primers TUN1 F5 and gp6 R) and
96 Fragment 2 gp9 (primer pair TUN1 gp9 F + R2). For TUN1 Δhpgc3 construction, the primer TUN1 gp9 R
97 and gp12 F were used instead of primer TUN1 2R and 3F, respectively, resulting in the new amplicons
98 Fragment 2 gp9_2 and Fragment 3 gp12 (Supplementary Figure S1D). In each case, TUN1 WT gDNA
99 was used as a PCR template.

100 To generate the triple mutant TUN1 Δhpgc123, Fragment 3 and Fragment 4 were amplified from TUN1
101 WT gDNA using the primer pairs mentioned above. Amplification of modified Fragment 1 was achieved
102 by using the primers TUN1 F5 and gp6 R and gDNA of TUN1 Δhpgc1 as a PCR template. Furthermore,

103 Fragment 2 was amplified from TUN1 Δhpgc2 gDNA by using the primer pair TUN1 gp9 F + R2
104 (Supplementary Figure S1E).

105 To construct rTUN1::*nLuc* either TUN1 WT or TUN1 Δ*gp7-8* gDNA was used as a PCR template. In both
106 cases, four fragments (F 5_1, 2, 3 and 4) were amplified using the primers TUN1 fwd5 + TUN1 rev1,
107 TUN1 fwd2+ rev2, TUN1 fwd3 + TUN1 MajCap rev, TUN1 MinCap fwd + TUN1 rev4. *nLuc* was amplified
108 from pNL2.1 (Promega, Walldorf, Germany) using the primer pair nLuc IGR Cap fwd/rev.

109 For all approaches DNA-Assembly was conducted using the NEBuilder DNA-Assembly Master Mix (New
110 England Biolabs, Ipswich, USA) according to the manufacturer's protocol. Oligonucleotide sequences
111 are listed in Supplementary Table S1. Primer design and *in-silico* cloning was carried out using Geneious
112 Prime (Version 2021.1.1, Biomatters New Zealand)

113 **Phage rebooting**

114 Phage assembly and rebooting was achieved in a non-replicative host by transforming chemically
115 competent *E. coli* 10-beta cells (New England Biolabs) with 5 µl of the assembly mix according to the
116 protocol provided by the manufacturer. After transformation 950 µl of LB medium were added and
117 the cells grown for 2 hours at 37° C with horizontal shaking at 120 rpm. Subsequently, the cells were
118 harvested for 5 min at 3,000 x g and the supernatant, containing rebooted phages, stored at 4° C until
119 further use.

120 **Plaque-Assay**

121 To check for functionality of (recombinant) TUN1 a fresh culture of *Kp* was grown to OD_{600}= 0.4-0.6
122 and then 350 µl of the culture were mixed with 2.5 ml hand-warm soft-agar [LB + 0.6 % Agar (w/v)]
123 together with 100 µl of phage stock/ transformation supernatant. Then, the mixture was evenly
124 distributed on a LB-agar plate and, after solidification, the plates were incubated at 37° C for 16 h. The
125 next day, plaque forming units (PFUs) were calculated and plaque morphology analyzed.

126 **Bacterial growth**

127 To determine the bacteriolytic activity of TUN1 phages on *Kp* strains, bacterial growth was measured
128 comparing samples with and without phages. For this purpose, 100 µl of the respective *Kp* culture (10^7
129 CFUs/ml) were mixed with either 100 µl of TUN1 phage stock ($1x10^3$ PFUs/ml) or 100 µl of LB medium
130 as a control in a 96-well plate with clear bottom. Plates were incubated at 37° C with shaking and
131 bacterial growth (OD_{600nm}) was measured every 30 min.

132 **rTUN1::*nLuc* functionality**

133 To measure luciferase activity on plaque containing LB-agar plates, 5 µl of the diluted (1:50, in PBS)
134 NanoLuc® luciferase substrate 2-furyl methyl-deoxy-coelenterazine (Furimazine; Promega) were
135 dropped onto the respective plaques. After incubation at RT for 3 min, the plates were analyzed for
136 luminescence signals using a ChemiDoc Imaging System and Image Lab 6.0.1 software (Bio-Rad
137 Laboratories Inc., Hercules, USA). Exposure time was set to 5 sec. The obtained luminescence signals
138 were then merged with an image of the plate for identification of plaques featuring luciferase activity.

139 To analyze luminescence in liquid culture medium over time, 100 µl of a fresh *Kp* culture ($1x10^7$ – 1
140 CFUs/ml) mixed with 100 µl of rTUN1::*nLuc* stock ($1x10^3$ PFUs/ml) were transferred into a cavity of a
141 96-well plate and supplemented with 2 µl of substrate. The plate was then incubated at 37° C under
142 continuous shaking (420 rpm) using a Varioskan Lux plate reader (Thermo Fisher Scientific, Waltham,
143 USA). Bacterial growth (OD_{600nm}) and luminescence (exposure time: 100 ms) were measured every 30
144 min for up to 16 h.

145 **Clinical matrices**

146 For rTUN1::*nLuc* based *Kp* detection in clinically relevant matrices, the reporter phage was added to
147 *Kp*-spiked urine and blood samples. Fresh urine was sterile filtered (0.22 µm luer lock syringe filter,
148 Merck Millipore, Cork, Ireland) spiked with the TUN1 host *Kp* 7984 (final conc. $1x10^7$ CFUs/ml).
149 Subsequently, bacterial growth and luminescence were measured in a plate reader every 30 min for 7
150 h at 37° C as described above.

151 To test the clinical matrix blood, 5 ml defibrinated sheep blood, spiked with the *Kp* 7984 (final conc.
152 $1x10^7$ CFUs/ml) was used. Prior to measurements, the serum was collected as described elsewhere
153 (Matsui et al., 2019). Briefly, the 5 ml spiked blood were injected into a 50 S-Monovette® (Sarstedt,
154 Nuernbrecht, Germany) and centrifuged at 2,000 x g for 15 min. The serum containing the bacterial
155 cells was then transferred into a fresh tube and centrifuged again. After discarding the supernatant,
156 the bacteria were resuspended to the original volume using LB medium. Subsequently, bacterial
157 growth and luminescence with and without the presence of rTUN1::*nLuc* was measured as described
158 above.

159 **Data analysis**

160 Sequence data was analyzed using Geneious Prime (Version 2021.1.1). All Varioskan data was analyzed
161 using the SkanIt 6.1 RE for Microplate Readers RE Software (Version 6.1.0.51) and GraphPad Prism
162 (Version 8.4.3).

163

164

Results

Successful rebooting of TUN1 from synthetic phage genomes requires circularized DNA

Generation of TUN1 (an Autographivirus featuring a 41 kb sized genome) reporter phages was aimed to be achieved by synthetic biology driven genetic engineering. As a proof of concept, the technical feasibility of *in vitro* assembly and phage rebooting had to be demonstrated prior to construction of reporter phages. For this, the TUN1 wildtype (WT) DNA was PCR amplified as five or four overlapping fragments and assembled *in vitro* generating linear or circularized synthetic phage genomes, respectively. Recombinant phage TUN1 was successfully rebooted by transforming the non-replicative host *E. coli* NEB Stable with circularized synthetic constructs while transformation of linear constructs did not result in any rebooted phages (Supplementary Figure S2). In a next step, we aimed at integrating the NanoLuc® luciferase gene (*nLuc*) fused to a ribosomal binding site (RBS) into the synthetic circular construct. As insertion site for the RBS-*nLuc* construct, the intergenic region between the major (*gp38*) and the minor (*gp39*) capsid genes was selected (Figure 1), as it qualifies for efficient transcription of the reporter due to the strong *cps* promoter regulating this operon (Loessner et al., 1996a). After *in vitro* DNA-aAssembly and phage rebooting, however, no plaques were observed on the *Kp* K64 strain 7984 indicating that no functional recombinant reporter phage particles had been generated. Thus, while recombinant phage can be assembled from DNA fragments and rebooted, a recombinant phage with the additional reporter gene *nLuc* cannot.

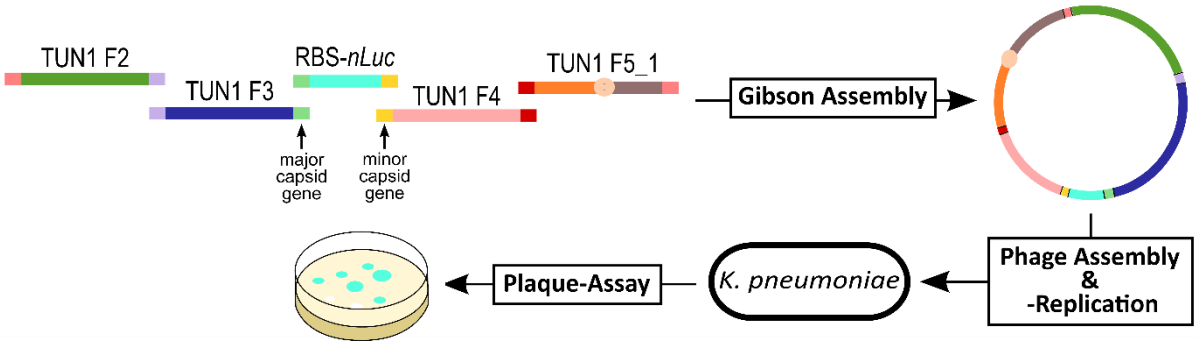

Figure 1. Schematic overview of TUN1 repoter phage construction. For construction of a TUN1 reporter phage all synthetic DNA fragments were amplified with overlapping ends between consecutive segments (depicted in matching colors). After *in vitro* DNA assembly the circular DNA was used to transform *E. coli* cells in which the recombinant phages were rebooted. Cells were lysed to release virions from the phage insusceptible host and the lysate used to infect *Kp*. Next, recombinant phage was *in vivo* amplified in its host *Kp* forming plaques on a lawn in the bacteria. Functional reporter phages were screened by measuring plaque luminescence after addition of luminogenic substrate.

Genome reduction of TUN1 enables insertion of *nLuc*-reporter

One possible explanation for unsuccessful reporter integration was that the capacity of DNA encapsulation in the nascent virion is already reached with the size of the WT genome of TUN1. To address this challenge, we next aimed to reduce the TUN1 WT genome to provide space for insertion of the *nLuc* construct. As TUN1 comprises multiple ORFs encoding proteins of unknown function

195 (Eckstein et al., 2021), these hypothetical genes (hpg) without any known function represent ideal
196 candidates for targeted gene deletion. We decided to eliminate the operons *gp2-4*, *gp7-8* and *gp10-*
197 *11* (Figure 2A) as these clusters were predicted to be regulated by single promoters, respectively. For
198 this, we used the same method as described for TUN1 WT *in vitro* assembly above but excluded the
199 selected hpg clusters (hpgc) during fragment amplification (Supplementary Figure S1), resulting in
200 TUN1 Δhpgc1, Δhpgc2 and Δhpgc3 featuring genome reductions by 518 bp, 529 bp and 738 bp,
201 respectively (Figure 2B). As all hpgc deletion variants resulted in functional phages, a triple deletion
202 strain (TUN1 Δhpgc123) was generated by using the single-cluster deletion mutants as PCR-templates
203 for subsequent synthetic phage genome rebooting. This resulted in a reduced genome size by 1,785
204 bp (Figure 2B). Analysis of the recombinant phages for their lytic activities against their host *Kp* 7984
205 in growth experiments, yielded no difference between TUN1 WT and the deletion variants (Figure 2C).
206 While the plaque sizes of TUN1 Δhpgc1 and Δhpgc2 on *Kp* 7984 were similar to that of TUN1 WT, those
207 of the deletion variants TUN1 Δhpgc3 and Δhpgc123 were slightly decreased. As the size of genome
208 reduction in TUN1 Δhpgc2 (529 bp) perfectly matched the size of the *nLuc* construct (526 bp) this
209 variant was used for reporter gene insertion in the next step.

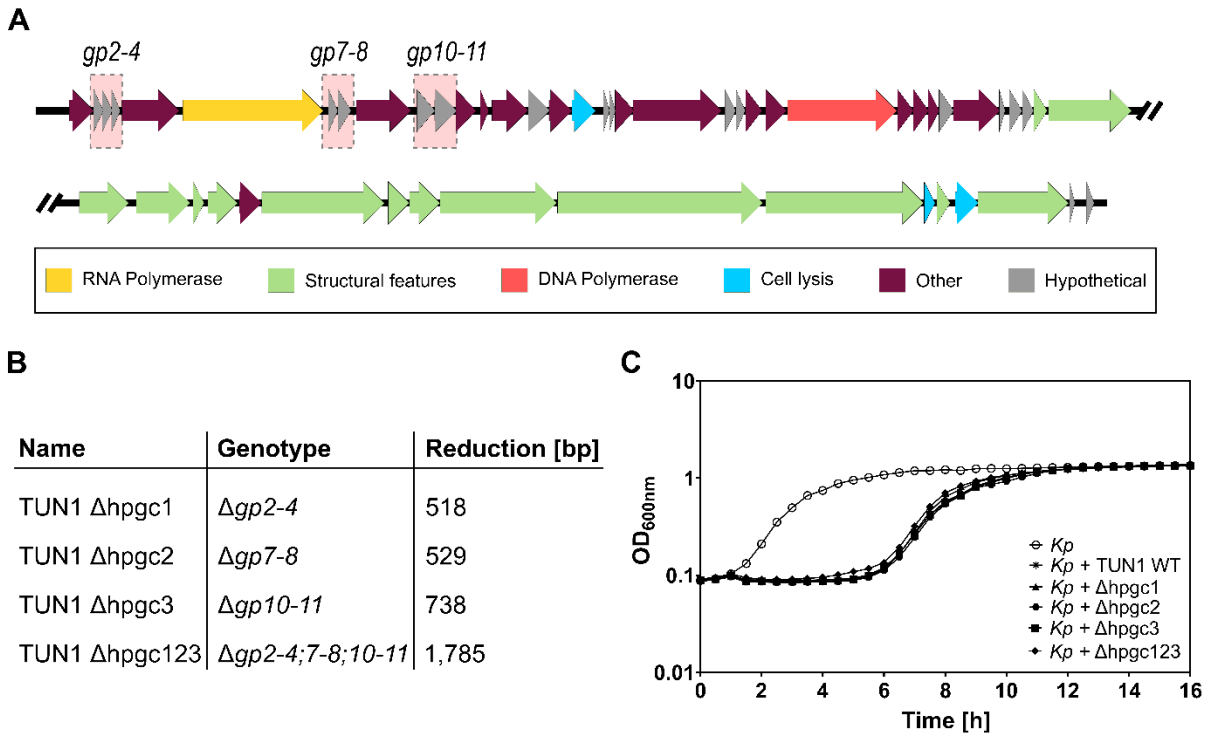

Name	Genotype	Reduction [bp]
TUN1 Δhpgc1	Δ*gp2-4*	518
TUN1 Δhpgc2	Δ*gp7-8*	529
TUN1 Δhpgc3	Δ*gp10-11*	738
TUN1 Δhpgc123	Δ*gp2-4;7-8;10-11*	1,785

210

211 **Figure 2**. **Characteristics of TUN1 deletion variants. A)** Schematic illustration of TUN1 genome. Hypothetical gene clusters
212 *gp2-4*, *gp7-8* and *gp10-11* are shaded in red. **B)** TUN1 deletion variants and their respective genome reduction. **C)** Growth
213 curves of *Kp* 7984 without phage (○), in the presence of TUN1 WT (∗), Δhpgc1 (▲), Δhpgc2 (●), Δhpgc3 (■) or Δhpgc123 (◆).

214 Using the genome-reduced TUN1 Δhpgc2 as a template, we were able to insert the *nLuc* construct and
215 thus to generate phage rTUN1::*nLuc.* Just like TUN1 WT and TUN1 Δhpgc2, rTUN1::*nLuc* also formed
216 distinct clear plaques surrounded by translucent halos when tested in plaque assay on *Kp* 7984. To

217 ascertain the functionality of the luciferase reporter, rTUN1::*nLuc* plaques were spot-covered with
218 furimazin, the substrate of NanoLuc® luciferase, and subsequently analyzed for luminescence. Indeed,
219 all plaques emitted light upon addition of furimazin (Figure 3) and therefore, rTUN1::*nLuc* can be used
220 for luminescence-based detection of *Kp* K64.

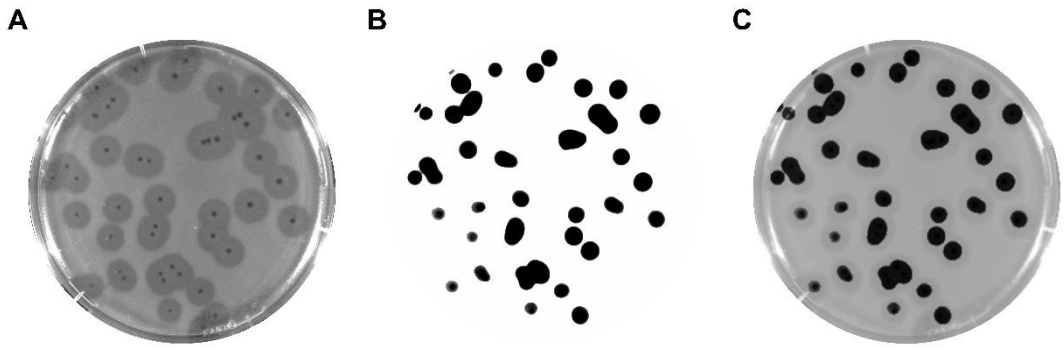

221

222 **Figure 3. Nanoluciferase activity of rTUN1::*nLuc* plaques. A**) Photographic image of a typical plaque assay agar plate with
223 recombinant reporter phage rTUN1::*nLuc* on *Kp* 7984 cells. **B**) Luminescent signal emitted from the agar plate (A) after
224 addition of luminogenic substrate (exposure time: 5 sec). **C**) Merged image of A and B.

225 **rTUN1::*nLuc* enables highly sensitive *Kp* K64 detection**

226 Plaque assays depend on bacterial growth on agar plates and are thus too time consuming for *Kp*
227 detection in clinical diagnostics. Therefore, the next step was to test the applicability of the reporter
228 phage rTUN1::*nLuc* for rapid luminescence-based *Kp* detection in liquid culture. For this, a liquid
229 culture of *Kp* 7984 ($1x10^6$ CFUs per well) was infected with $1x10^2$ PFUs (per well) of the reporter phage
230 and bacterial growth and luminescence were measured over time. We observed an immediate strong
231 increase of luminescence reaching a maximum of 10^8 relative light units (RLUs) after only 2 h of
232 incubation. This increase in luminescence correlated well with the start of impaired bacterial growth
233 compared to the control containing only *Kp* without rTUN1*::nLuc* (Figure 4A). Most probably caused
234 by autodegradation of the substrate, some luminescent background noise was also detected for *Kp*
235 7984 without phage. Therefore, the threshold for positive luminescence results was set to RLUs ≥ 10^3.
236 When different rTUN1::*nLuc* titers were tested, we observed high baseline luminescence (≥ 10^3 RLUs)
237 for phage titers greater than $1x10^3$ PFUs/well, even in phage-only control samples. This is most
238 probably due to carryover of NanoLuc® luciferase during preparation of rTUN1::*nLuc* phage stocks. An
239 initial titer of $1x10^2$ PFUs/well, on the other hand qualified as ideal phage concentration as the baseline
240 was comparable to the one produced by the no-phage control (Supplementary Figure S3).

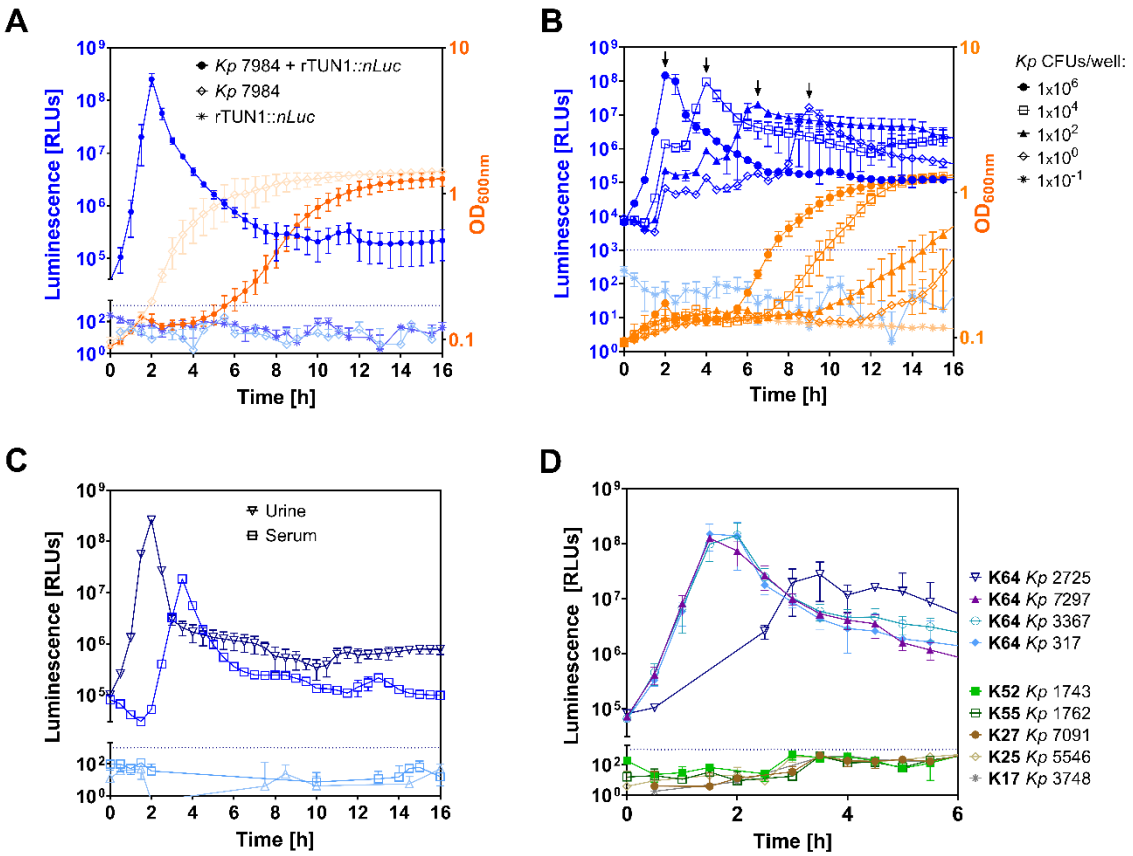

Figure 4. Luminescence based detection of *Kp* K64 using rTUN1::*nLuc*. A) Luminescence (blue) and bacterial growth (orange) measured for *Kp* 7984 ($1x10^6$ CFUs/well with (●) and without rTUN1::*nLuc* (◇) as well as solely rTUN1::*nLuc* (✱) over time. **B)** Luminescence (blue) and bacterial growth (orange) of different *Kp* 7984 concentrations per well (●: $1x10^6$ CFUs; □: $1x10^4$ CFUs; ▲: $1x10^2$ CFUs; ◇: $1x10^0$ CFU; ✱: $1x10^{-1}$ CFU) in the presence of rTUN1::*nLuc*. Black arrows (⬇) indicate the luminescence peaks generated by rTUN1::*nLuc* on respective bacterial culture. **C)** Luminescence for *Kp* 7984 + rTUN1::*nLuc* (dark blue) and without phage (light blue) in urine (▽) and serum (□). **D)** Luminescence of rTUN1::*nLuc* with *Kp* of different K-types (K64, K52, K55, K27, K25 and K17). For every experiment, an initial titer of 10^2 PFUs per well of the respective phage was used. Dotted blue line = threshold of 10^3 RLUs.

To investigate the sensitivity and thus the detection limit of the rTUN1::*nLuc* based reporter phage assay, a dilution series of *Kp* 7984 ($1x10^6$ – 0.1 CFUs per well) was tested using a starting concentration of $1x10^2$ PFUs/well of the reporter phage. Both the increase in detectable bacterial growth as well as the luminescence signal peak was delayed by 2-4 h with every dilution step. (Figure 4B). From this data a standard curve was generated which can be used to easily determine *Kp* concentrations based on the time of luminescence peak (Supplementary Figure S4). The results revealed that as few as one initial cell per well was sufficient to mediate yield a luminescent signal with its peak at 10^7 RLUs after approx. 9 hours. However, some of these wells with 10^0 *Kp* cells turned out negative (in luminescence and optical density) most probably because random distribution of single cells results in empty wells in some cases.

262 ***Kp* K64 cells can be detected directly in clinical matrices using rTUN1::*nLuc***

263 *Kp* can cause severe infections with fatal clinical outcomes, including UTI or sepsis. Therefore, urine
264 and blood represent relevant clinical matrices for *Kp* diagnostics. Using our reporter phage
265 rTUN1::*nLuc* on both *Kp*-spiked ($1x10^6$ CFUs/well) urine and blood samples, respectively, distinct
266 luminescence peaks could be measured. Conversely no matrix associated increase in background
267 luminescence was detected (Figure 4C). While the results for spiked urine samples were almost
268 identical to those measured in spiked growth medium, the luminescence peaks retrieved from spiked
269 blood samples appeared to be time-shifted by 2 h now correlating with the results of an initial *Kp*
270 concentration of $1x10^4$ CFUs/well. This can most easily be explained by a loss of 10^2 bacteria per ml
271 during serum collection from spiked blood.

272 **rTUN1::*nLuc* is highly specific for *Kp* K64 strains**

273 Recently, we described that TUN1 WT exclusively infects *Kp* K64 strains (Eckstein et al., 2021). In order
274 to verify the host specificity of rTUN1::*nLuc*, we analyzed the luminescence development in liquid
275 culture testing four additional *Kp* K64 strains and five *Kp* strains with other K-types (K55, K52, K27, K25
276 and K17) in the presence of the reporter phage. Positive signals (> 10^3 RLU) were obtained only from
277 samples containing *Kp* K64 strains indicating that rTUN1::*nLuc* features the same specificity for *Kp* K64
278 strains as the WT phage (Figure 4D).

279 **rTUN1::*nLuc* enables rapid, real-time antibiotic susceptibility testing of *Kp***

280 The main challenge for treatment of *Kp* infections is the increasing number of MDR *Kp* strains. For
281 instance, *Kp* 7984, the strain used in this work, has already been shown to be resistant to the first-line
282 AB ertapenem (Kollenda et al., 2019). Testing of antibiotic susceptibilities of *Kp* strains derived from
283 patient samples is therefore crucial to ensure successful therapy. However, these tests require a pure
284 culture of the infection-causing strain and often contain long incubation steps. To accelerate this
285 process of selecting the adequate ABs for an efficient therapy, we tested whether rTUN1::*nLuc* is also
286 suitable for the real-time, rapid AB susceptibility testing. For this, we used the experimental settings
287 of the luminescent reporter phage assay (10^6 CFUs/well *Kp* 7984 + 10^2 PFUs/well rTUN1::*nLuc,* shown
288 in Fig. 4A) and supplemented the growth medium with various ABs of different classes using their
289 minimal inhibitory concentration (MIC) at breakpoints determined for *Enterobacteriaceae*
290 (Supplementary Table S1). We observed no increase in reporter phage associated luminescence in the
291 presence of gentamicin (Gent), chloramphenicol (Cmp), imipenem (Imp), meropenem (Mer) and
292 amoxicillin/clavulanic acid (Amc) (Figure 5A). In contrast, we detected a strong luminescence increase
293 resulting in a distinct peak after 2 hours, comparable to that of the *Kp* 7984 + rTUN1::*nLuc*-control
294 without ABs, when levofloxacin (Lev), ceftazidim (Caz), streptomycin (Str), tigecyclin (Tgc+),
295 ciprofloxacin (Cip) and trimethoprim/sulfamethoxazol (T/S) had been added (Figure 5B). Growth
296 experiments of *Kp* 7984 (without phage) in the presence of ABs further revealed that Gent, Cmp, Imp,

297 Mer and Amc inhibited bacterial growth whereas *Kp* 7984 growth was not affected by the presence of
298 Caz, Str, Tgc+, Cip and T/S (Supplementary Figure S5). Thus, *Kp* 7984 can be considered sensitive to
299 Gent, Cmp, Imp, Mer and Amc and resistant to Caz, Str, Tgc+, Cip and T/S. In contrast to time consuming
300 classical growth experiments and MIC testing, our luminescent reporter phage assay using rTUN1::*nLuc*
301 not only enables rapid and sensitive detection of *Kp* K64 strains directly from clinical samples, but also
302 allows for simultaneous, real-time antibiotic susceptibility testing within just a few hours.

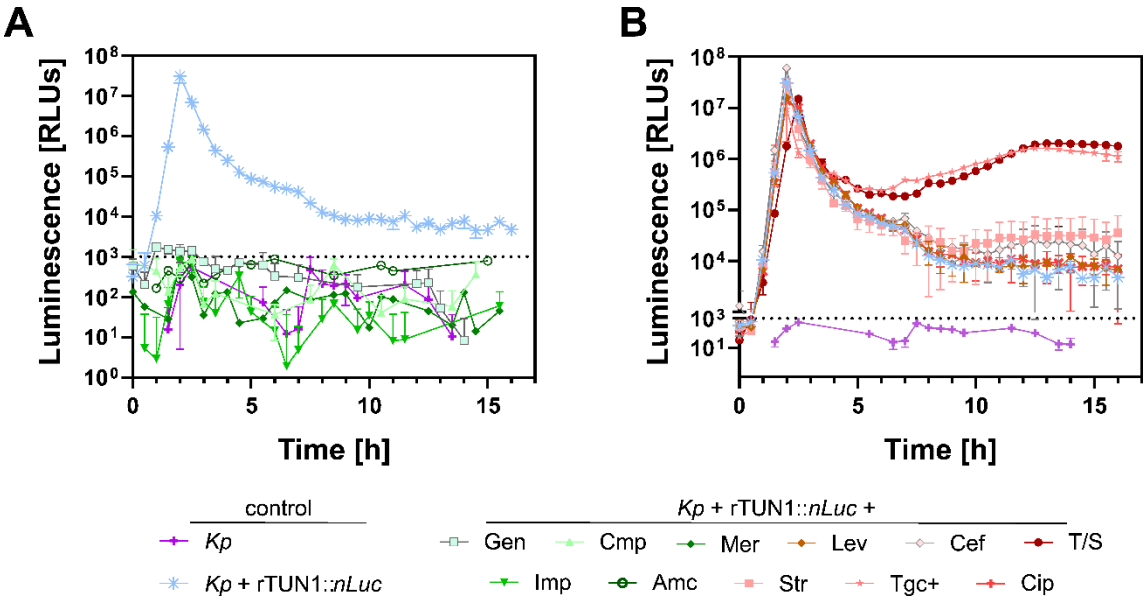

303

304 **Figure 5. Antibiotic susceptibility testing of *Kp* using rTUN1::*nLuc*.** Luminescence measurements of wells containing
305 rTUN1::*nLuc*-infected *Kp* 7984 ($1x10^6$ CFUs + $1x10^2$ PFUs per well) in the presence of different antibiotics. *Kp* without phage
306 (purple) and *Kp* + rTUN1::*nLuc* in pure LB (blue) served as controls **(A)** Despite the positive control no luminescence peak was
307 detected for wells containing *Kp* + rTUN1::*nLuc* in gentamicin (Gen), chloramphenicol (Cmp), imipenem (Imp), meropenem
308 (Mer) or amoxicillin/ clavulanic (Amc). **(B)** Distinct luminescence peaks were generated in samples containing *Kp* +
309 rTUN1::*nLuc* with levofloxacin (Lev), ceftazidime (Caz), streptomycin (Str), tigecyclin (Tgc+), ciprofloxacin (Cip) or
310 trimethoprim/ sulfamethoxazole (T/S). Error bars represent three independent biological replicates.
311

312

313 ## Discussion

314 The enormous increase of antibiotic resistances in bacteria has been estimated to lead to an excess
315 mortality of 10 million persons per year by 2050, mostly caused by nosocomial infections (Alebachew
316 Woldu, 2016; Borer et al., 2009). The multiple antibiotic resistance crisis constitutes a tremendous
317 threat to global health and has been declared a global health emergency (Toner et al., 2015) - a view
318 supported by WHO. Rapid pathogen detection and antibiotic resistance screening allows non-empirical
319 therapy and saves lifes. Established methods for *Kp* detection are time consuming and necessitate
320 empirical antibiotic therapy in urgent cases (Davenport et al., 2017) with more unfavorable outcomes.
321 Here, we demonstrated that reporter phage-based diagnostics could be a promising alternative, as
322 integration of reporter genes into highly specific phages enable real-time detection of phage
323 replication and thus, living host cells. Besides fluorescent proteins (Jain et al., 2012) and hydrolyzing

324 enzymes such as β-galactosidase (Chen et al., 2017; Chen et al., 2017)), luciferases can be used as
325 reporters (Hinkley et al., 2018; Loessner et al., 1996b; Meile, Sarbach, et al., 2020; Nguyen et al., 2017).

326 Since the discovery of luciferin-luciferase systems almost a century ago (McElroy & Ballentine, 1944),
327 several luciferase enzymes have become available to researchers. The latest commercially available
328 luciferase is the NanoLuc® enzyme (nLuc) which has several advantages compared to other luciferase
329 systems: It features a relatively small size of only 19.1 kDa (compared to e.g. the Renilla or Firefly
330 luciferase with 36 kDa or 61 kDa, respectively), fast substrate turnover rates - which leads to generation
331 of a high-intensity luminescent signal - and exhibits high stability under various buffer conditions
332 (England et al., 2016; Hall et al., 2012). Therefore, nLuc was selected as reporter candidate for this
333 study.

334 Inserting reporter genes, or any additional nucleotide sequence, into phage genomes can be
335 challenging. As DNA length and capsid size and thus internal pressure in the capsid correlate,
336 (Nurmemmedov et al., 2007) the DNA encapsulation capacity of most phages is limited. Hence,
337 integration of additional genes can negatively affect capsid stability and therefore lead to severe
338 impairments in phage assembly or replication (Grayson et al., 2006; Nurmemmedov et al., 2012). DNA
339 packaging of tailed phages relies on the recognition of specific sequences (*cos*- or *pac*-sites) by the
340 terminase protein followed by DNA cleavage. Depending on the phage type, this cleavage can be either
341 sequence-specific (e.g. T7 or λ) or nonspecific (e.g. P22 or SPP1). For the latter, the cleavage does not
342 occur at the end of the phage genome (so-called termination cleavage) but follows the mechanism of
343 headful packaging where nonspecific DNA cleavage by TerL (terminase large subunit) is induced by
344 increased capsid pressure. As a result, phages using the headful system often tolerate a genome size
345 of up to 110% while the others will not (Casjens & Gilcrease, 2009). Since TerL initiates DNA packaging
346 and cleavage, phylogenetic analysis of the *terl* gene can be used to predict a phage's DNA packaging
347 system. For TUN1, results of this analysis suggested that the phage belongs to the "T7-like group with
348 directed terminal repeats" and not to the "P22-like headful group". Therefore, the fact that our RBS-
349 *nLuc* reporter construct could not be inserted into the full-length TUN1 WT genome can most likely be
350 explained by its sequence-specific DNA packaging mechanism in combination with a genome size that
351 has already reached the maximum capsid capacity.

352 It has already been described, that insertion of additional genetic information into the genomes of
353 other *Podoviridiae* or *Autographiviridae* requires preceded genome reduction in order to overcome
354 the problem of limited capsid capacity (Kim et al., 2014; Pires et al., 2021). In this work, we were able
355 to minimize the TUN1 genome by up to 4.3 % (TUN1 Δhpgc123) and, at the same time, demonstrated
356 that the hypothetical genes *gp2-4*, *gp7-8* and *gp10-11* are not essential for a successful lytic cycle of
357 TUN1. Using the genome-reduced TUN1 Δhpgc2 as a template, insertion of the RBS-*nLuc* reporter

358 construct was successful. The resulting, luminescent reporter phage, rTUN1::*nLuc,* enabled specific and
359 ultrasensitive detection of *Kp* K64 cells exhibiting a limit of detection (LOD) of only CFU per well.

360 To our knowledge, there are only two other *Kp*-specific nLuc-based reporter phages, Mcoc and 8M7,
361 that specifically detect *Kp* K21 cells with a comparably low LOD of only 10 CFUs/well and 100 bacteria
362 per 100 mg feces, respectively (Zelcbuch et al., 2021). Other *nLuc*-based reporter phage assays
363 exhibited similar sensitivity. For instance, Pulkkinen et al constructed a T7-*nLuc* phage*,* which was able
364 to detect 47 *E. coli* cells per well (Pulkkinen et al., 2019). Further, ΦV10nluc phage-based *E. coli*
365 detection exhibited an even lower LOD of only 5 CFUs/well. These assays, however, were not tested
366 on clinically relevant matrices. In contrast, our novel rTUN1::*nLuc* based reporter phage assay enables
367 rapid detection of *Kp* cells from blood and urine samples exhibiting no matrix effects such as luciferase
368 quenching or unspecific increase in background luminescence. While the assay detected *Kp* K64 in
369 urine with the same sensitivity as pure bacterial culture, luminescence peaks retrieved from spiked
370 blood samples indicated a loss of bacterial cells during sample preparation. This was most probably
371 caused by the washing steps during serum collection rather than by blood associated matrix effects as
372 comparable studies have shown that similar optimization steps (serum separation and washing) of
373 spiked blood samples resulted in a 20-50% reduction in bacterial concentration (Moses et al., 2021;
374 Sergueev et al., 2017).

375 The current cutoff for diagnosis of UTIs, one of the most common diseases caused by *Kp,* is $1x10^5$
376 CFUs/ml urine (Becknell et al., 2015). Using our novel reporter phage assay, this minimal pathological
377 *Kp* load can be detected within four hours directly from the patient's urine. Compared to goldstandard
378 methods like PCR, rTUN1::*nLuc* only detects viable *Kp* cells, which can be crucial, e.g., for monitoring
379 therapy success where differentiation between living and dead cells is essential.

380 In addition to that, our approach allows for rapid, real-time assessment of antibiotic resistances (real-
381 time antibiogram) and thus, facilitates treatment of *Kp* K64 infections. Here, susceptibility against
382 therapeutically relevant antibiotics can be tested simultaneously to initial *Kp* detection from clinical
383 samples providing vital information for assessing treatment options in a few hours (depending on the
384 *Kp* load in the sample). In case of an infection with a MDR *Kp* K64 strain with no promising treatment
385 options left, rTUN1::*nLuc* can also function as a companion phage for phage therapy, as positive
386 luminescence readout from reporter phage assays also indicate infectivity of the wildtype TUN1 and
387 thus, qualifies for phage therapy.

388 In conclusion, our results clearly demonstrate the enormous diagnostic capabilities of reporter phages.
389 However, for broad applicability directly from clinical samples, such as urine from patients suffering
390 from UTIs, reporter phages need to be constructed not only for all locally occurring *Kp* K types, but for
391 all clinically relevant pathogens. This would then allow not only the rapid identification of the infection-

392 causing bacterial strain from unknown samples within a few hours, but also the simultaneous
393 generation of a real-time antibiogram of the infection-causing strain as well as the selection of
394 potential candidates for phage therapy.

395

396 ## References

397 ## Acknowledgements

398 We are grateful to Prof. Dr. Ben Moussa from the Military Hospital of Instruction in Tunis, for providing
399 the waste water samples from which we could initially isolate the bacteriophage TUN1.

400 ## Funding

401 This study was funded by the Medical Biological Defense Research Program of the Bundeswehr
402 Medical Service and supported by supported by the Enable and Enhance Initiative of the federal
403 government of Germany (Ertüchtigungsinitiative der Deutschen Bundesregierung, grant no. OR12-
404 370.43 ERT TUN IMB).

405 ## Authors' contribution

406 Conceptualization: S.E., J.J.B -and P.B.; investigation: R.R., P.B. and S.E.; methodology: S.E. and P.B.;
407 formal analysis and validation: P.B., R.R. and S.E.; visualization: S.E.; writing—original draft
408 preparation: S.E. and P.B.; writing—review and editing: P.B., J.J.B. and S.E.; supervision and project
409 administration: JJ.B. and S.E. All authors have read and agreed to the published version of the
410 manuscript.

411 ## References

412 Alebachew Woldu, M. (2016). Klebsiella pneumoniae and Its Growing Concern in Healthcare Settings.
413 *Clinical and Experimental Pharmacology*, *06*(01). https://doi.org/10.4172/2161-
414 1459.1000199

415 Anany, H., Brovko, L., El Dougdoug, N. K., Sohar, J., Fenn, H., Alasiri, N., Jabrane, T., Mangin, P.,
416 Monsur Ali, M., Kannan, B., Filipe, C. D. M., & Griffiths, M. W. (2018). Print to detect: A rapid
417 and ultrasensitive phage-based dipstick assay for foodborne pathogens. *Analytical and*
418 *Bioanalytical Chemistry*, *410*(4), 1217–1230. https://doi.org/10.1007/s00216-017-0597-y

419 Babini, G. S., & Livermore, D. M. (2000). Antimicrobial resistance amongst Klebsiella spp. Collected
420 from intensive care units in Southern and Western Europe in 1997–1998. *Journal of*
421 *Antimicrobial Chemotherapy*, *45*(2), 183–189. https://doi.org/10.1093/jac/45.2.183

422 Becknell, B., Schober, M., Korbel, L., & Spencer, J. D. (2015). The diagnosis, evaluation and treatment
423 of acute and recurrent pediatric urinary tract infections. *Expert Review of Anti-Infective*
424 *Therapy*, *13*(1), 81–90. https://doi.org/10.1586/14787210.2015.986097
425 Bhattacharya, S. (2013). Early diagnosis of resistant pathogens: How can it improve antimicrobial
426 treatment? *Virulence*, *4*(2), 172–184. https://doi.org/10.4161/viru.23326
427 Blasco, R., Murphy, M. J., Sanders, M. F., & Squirrell, D. J. (1998). Specific assays for bacteria using
428 phage mediated release of adenylate kinase. *Journal of Applied Microbiology*, *84*(4), 661–
429 666. https://doi.org/10.1046/j.1365-2672.1998.00393.x
430 Borer, A., Saidel-Odes, L., Riesenberg, K., Eskira, S., Peled, N., Nativ, R., Schlaeffer, F., & Sherf, M.
431 (2009). Attributable Mortality Rate for Carbapenem-Resistant *Klebsiella pneumoniae*
432 Bacteremia. *Infection Control & Hospital Epidemiology*, *30*(10), 972–976.
433 https://doi.org/10.1086/605922
434 Casjens, S. R., & Gilcrease, E. B. (2009). Determining DNA packaging strategy by analysis of the
435 termini of the chromosomes in tailed-bacteriophage virions. *Methods in Molecular Biology*
436 *(Clifton, N.J.)*, *502*, 91–111. https://doi.org/10.1007/978-1-60327-565-1_7
437 Chen, J., Alcaine, S. D., Jackson, A. A., Rotello, V. M., & Nugen, S. R. (2017). Development of
438 Engineered Bacteriophages for *Escherichia coli* Detection and High-Throughput Antibiotic
439 Resistance Determination. *ACS Sensors*, *2*(4), 484–489.
440 https://doi.org/10.1021/acssensors.7b00021
441 Chen, J., Picard, R. A., Wang, D., & Nugen, S. R. (2017). Lyophilized Engineered Phages for *Escherichia*
442 *coli* Detection in Food Matrices. *ACS Sensors*, *2*(11), 1573–1577.
443 https://doi.org/10.1021/acssensors.7b00561
444 Davenport, M., Mach, K. E., Shortliffe, L. M. D., Banaei, N., Wang, T.-H., & Liao, J. C. (2017). New and
445 developing diagnostic technologies for urinary tract infections. *Nature Reviews. Urology*,
446 *14*(5), 296–310. https://doi.org/10.1038/nrurol.2017.20

447 Domenico, P., Salo, R. J., Cross, A. S., & Cunha, B. A. (1994). Polysaccharide capsule-mediated
448 resistance to opsonophagocytosis in Klebsiella pneumoniae. *Infection and Immunity*, *62*(10),
449 4495–4499. https://doi.org/10.1128/iai.62.10.4495-4499.1994
450 Eckstein, S., Stender, J., Mzoughi, S., Vogele, K., Kühn, J., Friese, D., Bugert, C., Handrick, S., Ferjani,
451 M., Wölfel, R., Millard, A., Ben Moussa, M., & Bugert, J. J. (2021). Isolation and
452 characterization of lytic phage TUN1 specific for Klebsiella pneumoniae K64 clinical isolates
453 from Tunisia. *BMC Microbiology*, *21*(1), 186. https://doi.org/10.1186/s12866-021-02251-w
454 England, C. G., Ehlerding, E. B., & Cai, W. (2016). NanoLuc: A Small Luciferase Is Brightening Up the
455 Field of Bioluminescence. *Bioconjugate Chemistry*, *27*(5), 1175–1187.
456 https://doi.org/10.1021/acs.bioconjchem.6b00112
457 Garcia, E., Chain, P., Elliott, J. M., Bobrov, A. G., Motin, V. L., Kirillina, O., Lao, V., Calendar, R., &
458 Filippov, A. A. (2008). Molecular characterization of L-413C, a P2-related plague diagnostic
459 bacteriophage. *Virology*, *372*(1), 85–96. https://doi.org/10.1016/j.virol.2007.10.032
460 Goodridge, L., Chen, J., & Griffiths, M. (1999). Development and Characterization of a Fluorescent-
461 Bacteriophage Assay for Detection of *Escherichia coli* O157:H7. *Applied and Environmental*
462 *Microbiology*, *65*(4), 1397–1404. https://doi.org/10.1128/AEM.65.4.1397-1404.1999
463 Grayson, P., Evilevitch, A., Inamdar, M. M., Purohit, P. K., Gelbart, W. M., Knobler, C. M., & Phillips, R.
464 (2006). The effect of genome length on ejection forces in bacteriophage lambda. *Virology*,
465 *348*(2), 430–436. https://doi.org/10.1016/j.virol.2006.01.003
466 Hall, M. P., Unch, J., Binkowski, B. F., Valley, M. P., Butler, B. L., Wood, M. G., Otto, P., Zimmerman,
467 K., Vidugiris, G., Machleidt, T., Robers, M. B., Benink, H. A., Eggers, C. T., Slater, M. R.,
468 Meisenheimer, P. L., Klaubert, D. H., Fan, F., Encell, L. P., & Wood, K. V. (2012). Engineered
469 Luciferase Reporter from a Deep Sea Shrimp Utilizing a Novel Imidazopyrazinone Substrate.
470 *ACS Chemical Biology*, *7*(11), 1848–1857. https://doi.org/10.1021/cb3002478
471 Hartman, L. J., Selby, E. B., Whitehouse, C. A., Coyne, S. R., Jaissle, J. G., Twenhafel, N. A., Burke, R. L.,
472 & Kulesh, D. A. (2009). Rapid real-time PCR assays for detection of Klebsiella pneumoniae
473 with the rmpA or magA genes associated with the hypermucoviscosity phenotype: Screening

474 of nonhuman primates. *The Journal of Molecular Diagnostics: JMD*, *11*(5), 464–471.
475 https://doi.org/10.2353/jmoldx.2009.080136
476 Hennes, K. P., & Simon, M. (1995). Significance of bacteriophages for controlling bacterioplankton
477 growth in a mesotrophic lake. *Applied and Environmental Microbiology*, *61*(1), 333–340.
478 https://doi.org/10.1128/aem.61.1.333-340.1995
479 Herridge, W. P., Shibu, P., O'Shea, J., Brook, T. C., & Hoyles, L. (2020). Bacteriophages of Klebsiella
480 spp., their diversity and potential therapeutic uses. *Journal of Medical Microbiology*, 19.
481 Hinkley, T. C., Singh, S., Garing, S., Le Ny, A.-L. M., Nichols, K. P., Peters, J. E., Talbert, J. N., & Nugen,
482 S. R. (2018). A phage-based assay for the rapid, quantitative, and single CFU visualization of
483 E. coli (ECOR #13) in drinking water. *Scientific Reports*, *8*(1), 14630.
484 https://doi.org/10.1038/s41598-018-33097-4
485 Jain, P., Hartman, T. E., Eisenberg, N., O'Donnell, M. R., Kriakov, J., Govender, K., Makume, M., Thaler,
486 D. S., Hatfull, G. F., Sturm, A. W., Larsen, M. H., Moodley, P., & Jacobs, W. R. (2012). φ^{2}
487 GFP10, a High-Intensity Fluorophage, Enables Detection and Rapid Drug Susceptibility Testing
488 of Mycobacterium tuberculosis Directly from Sputum Samples. *Journal of Clinical*
489 *Microbiology*, *50*(4), 1362–1369. https://doi.org/10.1128/JCM.06192-11
490 Kim, S., Kim, M., & Ryu, S. (2014). Development of an Engineered Bioluminescent Reporter Phage for
491 the Sensitive Detection of Viable *Salmonella* Typhimurium. *Analytical Chemistry*, *86*(12),
492 5858–5864. https://doi.org/10.1021/ac500645c
493 Knothe, H., Shah, P., Krcmery, V., Antal, M., & Mitsuhashi, S. (1983). Transferable resistance to
494 cefotaxime, cefoxitin, cefamandole and cefuroxime in clinical isolates of Klebsiella
495 pneumoniae and Serratia marcescens. *Infection*, *11*(6), 315–317.
496 https://doi.org/10.1007/BF01641355
497 Kollenda, H., Frickmann, H., Helal, R. B., Wiemer, D. F., Naija, H., El Asli, M. S., Egold, M., Bugert, J. J.,
498 Handrick, S., Wölfel, R., Barguellil, F., & Moussa, M. B. (2019). Screening for carbapenemases
499 in ertapenem-resistant *Enterobacteriaceae* collected at a Tunisian hospital between 2014

500 and 2018. *European Journal of Microbiology and Immunology*, *9*(1), 9–13.
501 https://doi.org/10.1556/1886.2018.00033
502 Kurupati, P., Chow, C., Kumarasinghe, G., & Poh, C. L. (2004). Rapid Detection of *Klebsiella*
503 *pneumoniae* from Blood Culture Bottles by Real-Time PCR. *Journal of Clinical Microbiology*,
504 *42*(3), 1337–1340. https://doi.org/10.1128/JCM.42.3.1337-1340.2004
505 Loessner, M. J., Rees, C. E., Stewart, G. S., & Scherer, S. (1996a). Construction of luciferase reporter
506 bacteriophage A511::luxAB for rapid and sensitive detection of viable Listeria cells. *Applied*
507 *and Environmental Microbiology*, *62*(4), 1133–1140. https://doi.org/10.1128/aem.62.4.1133-
508 1140.1996
509 Loessner, M. J., Rees, C. E., Stewart, G. S., & Scherer, S. (1996b). Construction of luciferase reporter
510 bacteriophage A511::luxAB for rapid and sensitive detection of viable Listeria cells. *Applied*
511 *and Environmental Microbiology*, *62*(4), 1133–1140. https://doi.org/10.1128/aem.62.4.1133-
512 1140.1996
513 Matsui, A., Niimi, H., Uchiho, Y., Kawabe, S., Noda, H., & Kitajima, I. (2019). A Rapid ATP
514 Bioluminescence-based Test for Detecting Levofloxacin Resistance Starting from Positive
515 Blood Culture Bottles. *Scientific Reports*, *9*(1), 13565. https://doi.org/10.1038/s41598-019-
516 49358-9
517 McElroy, W. D., & Ballentine, R. (1944). The Mechanics of Bioluminescence. *Proceedings of the*
518 *National Academy of Sciences*, *30*(12), 377–382. https://doi.org/10.1073/pnas.30.12.377
519 Meile, S., Kilcher, S., Loessner, M. J., & Dunne, M. (2020). *Reporter Phage-Based Detection of*
520 *Bacterial Pathogens: Design Guidelines and Recent Developments*. 25.
521 Meile, S., Sarbach, A., Du, J., Schuppler, M., Saez, C., Loessner, M. J., & Kilcher, S. (2020). Engineered
522 Reporter Phages for Rapid Bioluminescence-Based Detection and Differentiation of Viable
523 Listeria Cells. *Applied and Environmental Microbiology*, *86*(11), 14.
524 Merino, S., Camprubí, S., Albertí, S., Benedí, V. J., & Tomás, J. M. (1992). Mechanisms of Klebsiella
525 pneumoniae resistance to complement-mediated killing. *Infection and Immunity*, *60*(6),
526 2529–2535. https://doi.org/10.1128/iai.60.6.2529-2535.1992

527 Moses, S., Vagima, Y., Tidhar, A., Aftalion, M., Mamroud, E., Rotem, S., & Steinberger-Levy, I. (2021).
528 Characterization of Yersinia pestis Phage Lytic Activity in Human Whole Blood for the
529 Selection of Efficient Therapeutic Phages. *Viruses*, *13*(1), 89.
530 https://doi.org/10.3390/v13010089
531 Nakano, R., Nakano, A., Ishii, Y., Ubagai, T., Kikuchi-Ueda, T., Kikuchi, H., Tansho-Nagakawa, S.,
532 Kamoshida, G., Mu, X., & Ono, Y. (2015). Rapid detection of the Klebsiella pneumoniae
533 carbapenemase (KPC) gene by loop-mediated isothermal amplification (LAMP). *Journal of*
534 *Infection and Chemotherapy*, *21*(3), 202–206. https://doi.org/10.1016/j.jiac.2014.11.010
535 Nguyen, C., Makkar, R., Sharp, N. J., Page, M. A., Molineux, I. J., & Schofield, D. A. (2017). Detection of
536 Bacillus anthracis spores from environmental water using bioluminescent reporter phage.
537 *Journal of Applied Microbiology*, *123*(5), 1184–1193. https://doi.org/10.1111/jam.13569
538 Nobrega, F. L., Vlot, M., de Jonge, P. A., Dreesens, L. L., Beaumont, H. J. E., Lavigne, R., Dutilh, B. E., &
539 Brouns, S. J. J. (2018). Targeting mechanisms of tailed bacteriophages. *Nature Reviews*
540 *Microbiology*, *16*(12), 760–773. https://doi.org/10.1038/s41579-018-0070-8
541 Nurmemmedov, E., Castelnovo, M., Catalano, C. E., & Evilevitch, A. (2007). Biophysics of viral
542 infectivity: Matching genome length with capsid size. *Quarterly Reviews of Biophysics*, *40*(4),
543 327–356. https://doi.org/10.1017/S0033583508004666
544 Nurmemmedov, E., Castelnovo, M., Medina, E., Catalano, C. E., & Evilevitch, A. (2012). Challenging
545 Packaging Limits and Infectivity of Phage λ. *Journal of Molecular Biology*, *415*(2), 263–273.
546 https://doi.org/10.1016/j.jmb.2011.11.015
547 Pan, Y.-J., Lin, T.-L., Chen, C.-T., Chen, Y.-Y., Hsieh, P.-F., Hsu, C.-R., Wu, M.-C., & Wang, J.-T. (2015).
548 Genetic analysis of capsular polysaccharide synthesis gene clusters in 79 capsular types of
549 Klebsiella spp. *Scientific Reports*, *5*(1), 15573. https://doi.org/10.1038/srep15573
550 Patel, G., Huprikar, S., Factor, S. H., Jenkins, S. G., & Calfee, D. P. (2008). Outcomes of Carbapenem-
551 Resistant *Klebsiella pneumoniae* Infection and the Impact of Antimicrobial and Adjunctive
552 Therapies. *Infection Control & Hospital Epidemiology*, *29*(12), 1099–1106.
553 https://doi.org/10.1086/592412

554 Pires, D. P., Monteiro, R., Mil-Homens, D., Fialho, A., Lu, T. K., & Azeredo, J. (2021). Designing P.
555 aeruginosa synthetic phages with reduced genomes. *Scientific Reports*, *11*(1), 2164.
556 https://doi.org/10.1038/s41598-021-81580-2
557 Prestinaci, F., Pezzotti, P., & Pantosti, A. (2015). Antimicrobial resistance: A global multifaceted
558 phenomenon. *Pathogens and Global Health*, *109*(7), 309–318.
559 https://doi.org/10.1179/2047773215Y.0000000030
560 Pulkkinen, E. M., Hinkley, T. C., & Nugen, S. R. (2019). Utilizing in vitro DNA assembly to engineer a
561 synthetic T7 Nanoluc reporter phage for Escherichia coli detection. *Integrative Biology:*
562 *Quantitative Biosciences from Nano to Macro*, zyz005. https://doi.org/10.1093/intbio/zyz005
563 Schwaber, M. J., Klarfeld-Lidji, S., Navon-Venezia, S., Schwartz, D., Leavitt, A., & Carmeli, Y. (2008).
564 Predictors of Carbapenem-Resistant *Klebsiella pneumoniae* Acquisition among Hospitalized
565 Adults and Effect of Acquisition on Mortality. *Antimicrobial Agents and Chemotherapy*, *52*(3),
566 1028–1033. https://doi.org/10.1128/AAC.01020-07
567 Sergueev, K., Filippov, A., & Nikolich, M. (2017). Highly Sensitive Bacteriophage-Based Detection of
568 Brucella abortus in Mixed Culture and Spiked Blood. *Viruses*, *9*(6), 144.
569 https://doi.org/10.3390/v9060144
570 Shon, A. S., Bajwa, R. P. S., & Russo, T. A. (2013). Hypervirulent (hypermucoviscous) *Klebsiella*
571 *pneumoniae*: A new and dangerous breed. *Virulence*, *4*(2), 107–118.
572 https://doi.org/10.4161/viru.22718
573 Stewart, L. D., Foddai, A., Elliott, C. T., & Grant, I. R. (2013). Development of a novel phage-mediated
574 immunoassay for the rapid detection of viable *Mycobacterium avium* subsp.
575 *Paratuberculosis*. *Journal of Applied Microbiology*, *115*(3), 808–817.
576 https://doi.org/10.1111/jam.12275
577 Toner, E., Adalja, A., Gronvall, G.K., Cicero, A., Inglesby, T.V. (2015). Antimicrobial resistance is a
578 global health emergency. *Health Secur.* 2015 May-Jun;13(3):153-5. doi:
579 10.1089/hs.2014.0088. PMID: 26042858; PMCID: PMC4486712.
580

Turnbull, P.C. (2008) World Health Organization. Anthrax in humans and animals. In: (Editor) PT, editor. Geneva (CH): WHO Press.

Zelcbuch, L., Yitzhaki, E., Nissan, O., Gidron, E., Buchshtab, N., Kario, E., Kredo-Russo, S., Zak, N. B., & Bassan, M. (2021). Luminescent Phage-Based Detection of Klebsiella pneumoniae: From Engineering to Diagnostics. *Pharmaceuticals*, *14*(4), 347. https://doi.org/10.3390/ph14040347